Detailed Studies and Control of Intensity-Related Dynamics of Femtosecond Frequency Combs From Mode-Locked Ti:Sapphire Lasers

Kevin W. Holman, R. Jason Jones, Adela Marian, Steven T. Cundiff, and Jun Ye

***Abstract*—The authors have conducted detailed experimental investigations of the intensity-related dynamics of the pulse repetition and carrier-envelope offset frequencies of passively mode-locked Ti:sapphire lasers. Two different laser systems utilizing different intracavity dispersion compensation schemes are used in this study. Theoretical interpretations agree well with experimental data, indicating that intensity-related spectral shifts, coupled with the cavity group-delay dispersion, are important in understanding the dynamics of the frequency comb. Minimization of spectral shifts or the magnitude of group-delay dispersion leads to minimization of the intensity dependence of the femtosecond comb.**

***Index Terms*—Lasers, nonlinear optics, solid state lasers, ultrafast optics.**

I. Introduction

THE use of stabilized mode-locked femtosecond lasers has played a key role in the recent advances in optical frequency measurement [1], [2], carrier-envelope phase stabilization [3]–[5], optical clocks [6], [7], optical frequency synthesizers [8], laser synchronization [9], and pulse synthesis [10]. These various applications provide strong motivation to develop the ultrafast laser to be more reliable, more stable, and easier to control. Conversely, with the aid of precision measurement tools, we can enhance understanding of the mode-locking mechanism and dynamics of the laser.

Currently, the most versatile and reliable ultrafast lasers are Kerr-lens mode-locked Ti:sapphire (Ti:s) systems. For these lasers, there are two basic schemes that compensate for the cavity group-delay dispersion (GDD) and therefore allow for the generation of ultrashort pulses. One utilizes an intracavity prism pair, while the other takes advantage of negatively chirped mirrors. The latter system typically enables a reduced cavity length at the expense of fixed intracavity GDD. In this work, we use both a prism-based laser system with a repetition rate of 100 MHz [11], and a prismless laser with a 750-MHz repetition rate [12]. Both laser systems have successfully produced octave-bandwidth optical frequency combs when broadened using microstructure fibers [13]. Compared with the 100-MHz laser, the reduced energy per pulse in the 750-MHz laser requires a higher average power and an increased nonlinear interaction length for the continuum generation. On the other hand, the 750-MHz laser has a higher power per comb mode and, therefore, can produce a larger signal-to-noise ratio (S/N) in heterodyne detection of one of the comb lines with a cw laser. The 750-MHz laser is also attractive in frequency metrology due to its easier-to-identify comb mode orders with a larger spacing.

There are two degrees of freedom associated with the optical comb [14], [15]: the laser repetition frequency $(f_{\rm rep})$ and the carrier-envelope offset frequency $(f_{\rm ceo})$, where $f_{\rm rep} = v_g/l_c$ and $f_{\rm ceo} = (\omega_c/2\pi)(1 - v_g/v_p)$. ω_c is the spectrally weighted center frequency, l_c is the round-trip cavity length, and $v_g(v_p)$ is the average group (phase) velocity inside the cavity. The absolute frequency of each comb line is given by $f_m = mf_{\rm rep}+f_{\rm ceo}$. In the time domain, the pulse-to-pulse carrier-envelope phase shift is expressed as $\Delta\phi = 2\pi f_{\rm ceo}/f_{\rm rep} = \omega_c l_c(1/v_g - 1/v_p)$. For experiments sensitive to the carrier-envelope phase, fluctuations in $\Delta\phi$ can often be stabilized by controlling the pump laser power [3], which influences both v_g and v_p differently. For example, strong-field processes such as high-order harmonic emission are sensitive to this phase for short pulses which comprise only a few optical cycles [16], [17]. Using an acousto-optic modulator (AOM) in the pump beam path to control the pumping power, $f_{\rm ceo}$ can be locked to zero, thereby stabilizing $\Delta\phi$ to zero. A servo bandwidth $\geq$100 kHz can be achieved. A high-speed servo will be particularly useful for taking advantage of the high signal-to-noise ratio of the error signal when stabilizing a femtosecond laser comb to an external optical cavity [18]. On the other hand, in some schemes for implementing an optical clock it is only necessary to stabilize $f_{\rm rep}$ [7]. For frequency metrology applications the comb spectrum needs to be stabilized absolutely, and both degrees of freedom need to be stabilized. In this case, $f_{\rm rep}$ can be controlled with the cavity length, l_c. Changes in the cavity length have a minimal effect on $f_{\rm ceo}$ as v_g/v_p is only slightly modified, which is verified in practice [19].

Previous work has attributed the dominant source of noise in $f_{\rm ceo}$ to power fluctuations, explained in terms of spectral shifts [3], self-steepening, and nonlinear refraction [20]. In this paper, we report detailed experimental investigations of intensity-related dynamics in both the repetition and the carrier-envelope offset frequencies for both laser systems. We observe for the first time an interesting sign reversal in the dependence

Manuscript received January 16, 2003; revised May 29, 2003. This work was supported in part by the Office of Naval Research, NASA, the National Science Foundation, and the National Institute of Standards and Technology. K. Holman is a Hertz Foundation Graduate Fellow. R. J. Jones is a National Research Council Postdoctoral Fellow.

The authors are with JILA, National Institute of Standards and Technology and the Department of Physics, University of Colorado, Boulder, CO 80309 USA (e-mail: kevin.holman@colorado.edu; rjjones@jilau1.colorado.edu; adela.marian@colorado.edu; cundiffs@jila.colorado.edu; ye@jila.colorado.edu).

Digital Object Identifier 10.1109/JSTQE.2003.819098

of $f_{\rm rep}$ and $f_{\rm ceo}$ on the laser power. These dynamics are explained by a corresponding shift in the spectrum of the laser pulse. Mode-locking conditions are found under which the intensity-related spectral shift or the magnitude of GDD is minimized, leading to minimization of the noise of both $f_{\rm rep}$ and $f_{\rm ceo}$. This new understanding has strong implications on the optimal use of the pump power to control the phase of femtosecond lasers.

II. Theoretical Calculations of Intensity Dependence of Femtosecond Comb Parameters

The dependence of the frequencies $f_{\rm ceo}$ and $f_{\rm rep}$ on the pulse peak intensity I (and hence the laser power) can be found by differentiating the expressions for $f_{\rm ceo}$ and $f_{\rm rep}$ with respect to I

$$\frac{df_{\rm rep}}{dI} = \frac{1}{l_c}\frac{dv_g}{dI} \tag{1a}$$

$$\frac{df_{\rm ceo}}{dI} = \frac{1}{2\pi}\frac{\partial\omega_c}{\partial I}\left(1-\frac{v_g}{v_p}\right)+\frac{\omega_c}{2\pi}\frac{v_g}{v_p}\left(\frac{1}{v_p}\frac{dv_p}{dI}-\frac{1}{v_g}\frac{dv_g}{dI}\right). \tag{1b}$$

Here, $\partial\omega_c/\partial I$ is the intensity-related laser spectral shift. Denote $\overline{n}(\overline{n}=\overline{n}_0+\overline{n}_2 I)$ as the average refractive index in the laser cavity, so that the product $(\overline{n}l_c)$ is equivalent to the true optical path distance through the air and the Ti:s crystal during a cavity round trip. Then, $v_g = c/\left[\overline{n}+\omega_c\left(d\overline{n}/d\omega\right)_{\omega_c}\right]$ and $v_p = c/\overline{n}$. (From these expressions we note that v_g and v_p depend indirectly on l_c, since $\overline{n}$ is slightly modified when l_c changes.) This, then, leads to the following expressions for the dependence of $f_{\rm rep}$ and $f_{\rm ceo}$ on I. The appendix contains a detailed derivation of these relations

$$\frac{df_{\rm rep}}{dI} = -\frac{1}{l_c}\frac{v_g^2}{c}\left[\overline{n}_2+\omega_c\left(\frac{d\overline{n}_2}{d\omega}\right)_{\omega_c}+c\frac{\partial\omega_c}{\partial I}\frac{\partial}{\partial\omega_c}\left(\frac{1}{v_g}\right)\right] \tag{2}$$

$$\begin{aligned}\frac{df_{\rm ceo}}{dI} =& \frac{\omega_c^2}{2\pi}\frac{v_g^2}{c^2}\left[\overline{n}_0\left(\frac{d\overline{n}_2}{d\omega}\right)_{\omega_c}-\overline{n}_2\left(\frac{d\overline{n}_0}{d\omega}\right)_{\omega_c}\right]\\ &+\frac{1}{2\pi}\frac{\partial\omega_c}{\partial I}\left[\left(1-\frac{v_g}{v_p}\right)+\frac{\omega_c v_g^2}{v_p}\frac{\partial}{\partial\omega_c}\left(\frac{1}{v_g}\right)\right.\\ &\left.-\frac{\omega_c v_g}{c}\frac{\partial\overline{n}}{\partial\omega_c}\right].\end{aligned} \tag{3}$$

All terms in (2) and (3), except $\partial\omega_c/\partial I$ and $\partial(v_g^{-1})/\partial\omega_c$, are constants taken from the literature. The last term in (2) and the second set of brackets in (3) reveal the dependence on the intensity-related spectral shift. Both equations are dominated by the term proportional to $(\partial\omega_c/\partial I)(\partial(v_g^{-1})/\partial\omega_c)$, explaining the near coincidence in the sign change of $df_{\rm rep}/dI$ and $df_{\rm ceo}/dI$ with that of $\partial\omega_c/\partial I$. From the dependence of $f_{\rm rep}$ on the pulse peak intensity, given in (2), an experimental measurement of $df_{\rm rep}/dI$ and $\partial\omega_c/\partial I$ will uniquely determine the dependence of the average group velocity on the laser spectrum, namely, $\partial(v_g^{-1})/\partial\omega_c$. This value is then used in conjunction with $\partial\omega_c/\partial I$ to determine the dependence of $f_{\rm ceo}$ on the peak intensity, using (3), which can be compared with an experimental measurement of $df_{\rm ceo}/dI$.

In order to evaluate these expressions, several parameters are needed. The cavity-filling factor (ratio of Ti:s crystal length to overall cavity length) of the 750-MHz laser is needed to determine the average value of the linear refractive index and its dispersion. This filling factor is 0.006, yielding $\overline{n}_0 = 1.00456$ and $d\overline{n}_0/d\omega = 6\times10^{-20}[s]$ for the entire laser cavity. In the calculation of $d\overline{n}_0/d\omega$, the contribution by the mirrors to the linear dispersion is neglected. A rough estimation of the maximum contribution by one mirror, attributing the pulse delay to a reasonable dielectric mirror thickness, yields a negligible contribution to $d\overline{n}_0/d\omega$. For the nonlinear contribution, Gaussian beam propagation through the Ti:s crystal is taken into account, giving an effective cavity-filling factor of 0.0037. From this, we determine $\overline{n}_2\sim7.3\times10^{-23}[m^2W^{-1}]$, and $d\overline{n}_2/d\omega\sim1.2\times10^{-38}[sm^2W^{-1}]$, based on the value of $d\overline{n}_2/d\omega$ for Ti:s adopted from [20]. In order to convert from the experimentally measured values of the average output power to the quantity of interest, the pulse peak intensity, we need the following parameters relevant to the laser cavity: the beam waist inside the Ti:s crystal, 10 μm (20 μm) for the 750-MHz (100-MHz) laser; the output coupling, 3% (12%); and the pulse bandwidth, $\sim$22 nm (50 nm).

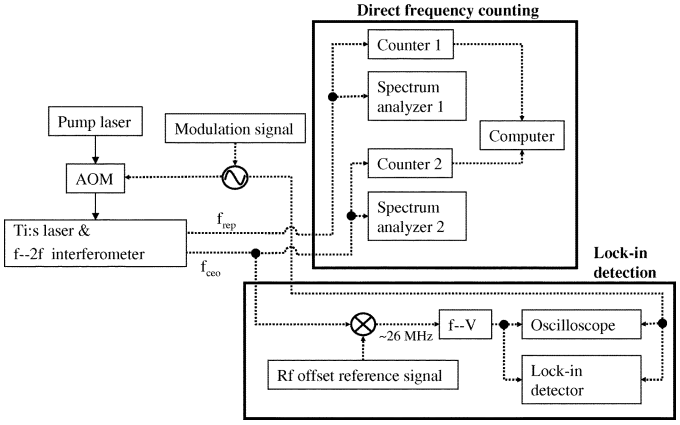

Fig. 1. Experimental setup for measurement of $f_{\rm rep}$ and $f_{\rm ceo}$ and their dynamics. Both direct frequency counting and lock-in detection are used.

III. Experimental Investigation of Intesity-Related Comb Dynamics

The values of $f_{\rm rep}$ and $f_{\rm ceo}$ and their intensity-related dynamics are determined by two approaches. For measurement of relatively slow changes and/or thermal responses, we use a direct-frequency-counting technique to track $f_{\rm rep}$ and $f_{\rm ceo}$. For measurement of dynamic responses at Fourier frequencies higher than a few tens of Hertz, we introduce sinusoidal modulation to the laser intensity and use subsequent lock-in detection. These two schemes are summarized in Fig. 1. In both scenarios, the intensity of the laser is modulated by an AOM in the path of the pump beam. The carrier-envelope offset frequency is detected with a $f-2f$ self-referencing interferometer [4]. For direct frequency counting, $f_{\rm rep}$ and $f_{\rm ceo}$ are recorded with two frequency counters working at appropriately chosen gate times. A radio frequency (rf) spectrum analyzer is utilized for analysis of spectral linewidth and shape, as well as easy readout of the mean values of the frequencies. For measurement of slow responses near dc, the laser intensity is modulated at about 0.1 Hz so that the frequency counters with a gate time of 0.1 s can track the changing frequencies with sufficient resolution and speed. For measurement of fast dynamics involving lock-in detection,

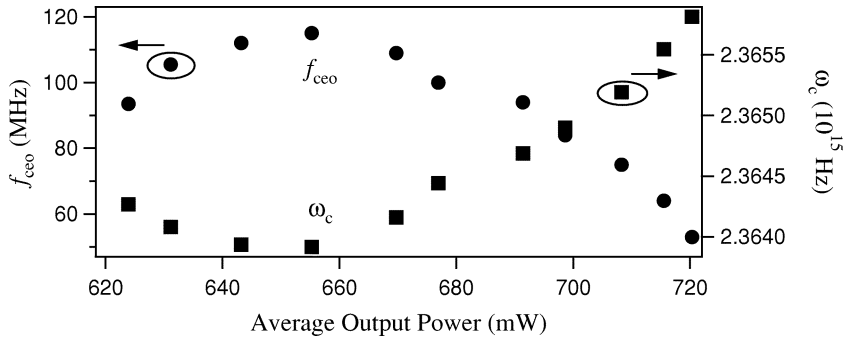

Fig. 2. Shift of ω_c and $f_{\rm ceo}$ with respect to the average output power of the 750-MHz laser. Squares, ω_c; circles, $f_{\rm ceo}$.

we mix the frequency signal of $f_{\rm ceo}$ with another stable rf reference to produce a heterodyne beat that falls within the input frequency range of a frequency-to-voltage (f–V) converter. The frequency response (transfer function) of the f–V converter is carefully measured so that the true response of the laser can be extracted from the raw data after removing the effect of the f-V converter. A lock-in detector and a fast digital oscilloscope are used to measure the modulation magnitude of $f_{\rm ceo}$ for modulation frequencies up to 400 kHz.

A. Intensity Dependence of Comb Parameters at DC

Fig. 2 illustrates intensity-related shifts of the center frequency of the pulse spectrum, ω_c, and the carrier-envelope offset frequency, $f_{\rm ceo}$, for the 750-MHz laser. We obtain these measurement results by slowly increasing (or decreasing) the laser pump power, without any fast modulations. The value of ω_c is determined from the weighted average of the pulse spectrum displayed on an optical spectrum analyzer. Under certain conditions, variation of the laser pump power may result in the emergence of cw lasing components in addition to the pulse spectrum. The cw frequency components inside the laser cavity can have a significant influence on the pulse dynamics. The ring-type cavity of the 750-MHz laser makes it straightforward to detect any existing cw components by monitoring the cavity output in the direction opposite to pulse propagation. The laser is carefully adjusted to ensure that no cw components are present within the range of power variation. An autocorrelation measurement also confirms that the pulse width remains constant within this same range. The measured changes of the laser responses can therefore be attributed entirely to mode-locking dynamics related to the pulse peak intensity. Fig. 2 proves clearly that neither ω_c, shown as squares with respect to the vertical axis at right, nor $f_{\rm ceo}$, displayed as circles, is a monotonic function of the laser power. In other words, there is a change in the sign of $df_{\rm ceo}/dI$, which is accompanied by a sign change of $\partial\omega_c/\partial I$. We use a second-order polynomial fit to the ω_c data, and experimental values of the intensity-related spectral shift $\partial\omega_c/\partial I$ are determined from the derivative of this fit.

DC values of $df_{\rm rep}/dI$ and $df_{\rm ceo}/dI$ are determined using the direct-frequency-counting method mentioned previously. Shown in Fig. 3 are some representative data of the slowly modulated carrier-envelope offset frequency (pluses) with fits to a sine function (solid lines) for various average values of the output power for the 750-MHz laser. These data were taken for laser powers below the zero crossing of $df_{\rm ceo}/dI$, i.e., before the sign change of $df_{\rm ceo}/dI$, and with roughly the same power modulation. Hence, as the laser power increases, the dc value of $f_{\rm ceo}$ increases while its modulation response amplitude decreases. The original raw data of $f_{\rm ceo}$ contained a linear drift that has been subtracted, since only the modulation amplitude is of interest. From the amplitudes of the sinusoidal fit and direct measurements of the modulation depth of the average output power, experimental values of $df_{\rm rep}/dI$ and $df_{\rm ceo}/dI$ are determined. These values are shown in Fig. 4, with filled circles for $df_{\rm rep}/dI$ and open circles for $df_{\rm ceo}/dI$. From the experimental values of $df_{\rm rep}/dI$ and $\partial\omega_c/\partial I$, we can determine the values of $\partial(v_g^{-1})/\partial\omega_c$ using (2). The values of $\partial(v_g^{-1})/\partial\omega_c$ are found to be negative, consistent with the fact that the linear contribution to the GDD in the laser cavity is negative in order to compensate for the positive nonlinear contribution to the GDD. The calculated values of $\partial(v_g^{-1})/\partial\omega_c$ are then used in conjunction with those of $\partial\omega_c/\partial I$ to compute $df_{\rm ceo}/dI$ via (3), with the results shown as triangles in Fig. 4. These calculated values of $df_{\rm ceo}/dI$ are in good agreement with the directly measured data, showing our data is self-consistent with (2) and (3).

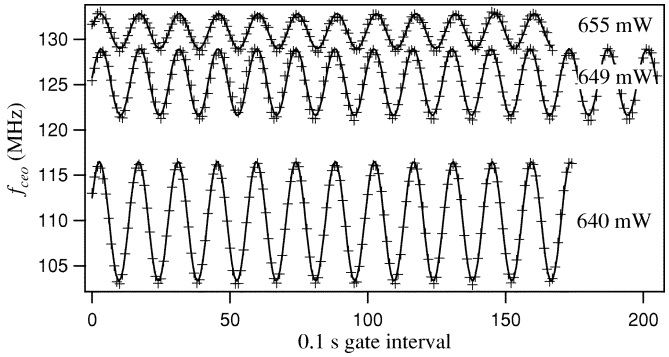

Fig. 3. Direct frequency counting of slow modulation of $f_{\rm ceo}$ for the 750-MHz laser for powers below zero-crossing point of $df_{\rm ceo}/dI$ (pluses), and sine function fits (solid lines). Modulation depth of power is roughly the same. DC value of $f_{\rm ceo}$ increases with power ($df_{\rm ceo}/dI > 0$), whereas modulation response decreases as it approaches zero crossing of $df_{\rm ceo}/dI$.

B. Dynamic Response of the Carrier-Envelope Offset Frequency

It is also interesting to study the dynamic response of $f_{\rm ceo}$, which is determined via the lock-in detection technique of Fig. 1. The modulation depth of $f_{\rm ceo}$ given by lock-in detection, along with direct measurement of the modulation amplitude of the output power, determines the dynamic response of

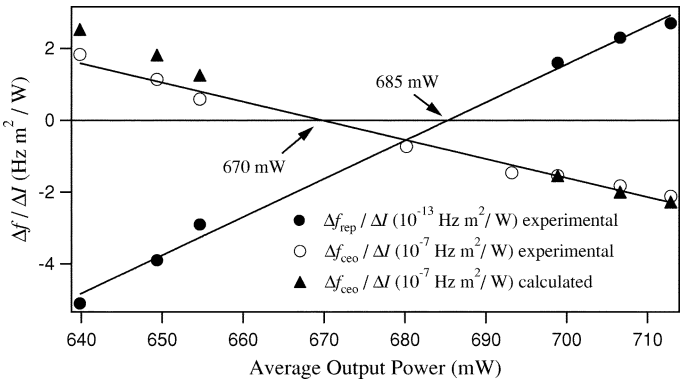

Fig. 4. Directly measured $\Delta f_{\rm rep}/\Delta I$ (filled circles) and $\Delta f_{\rm ceo}/\Delta I$ (open circles) versus the average output power of the 750 MHz laser. Calculated $\Delta f_{\rm ceo}/\Delta I$ based on a parameter derived from the measured $\Delta f_{\rm rep}/\Delta I$ data are shown as triangles.

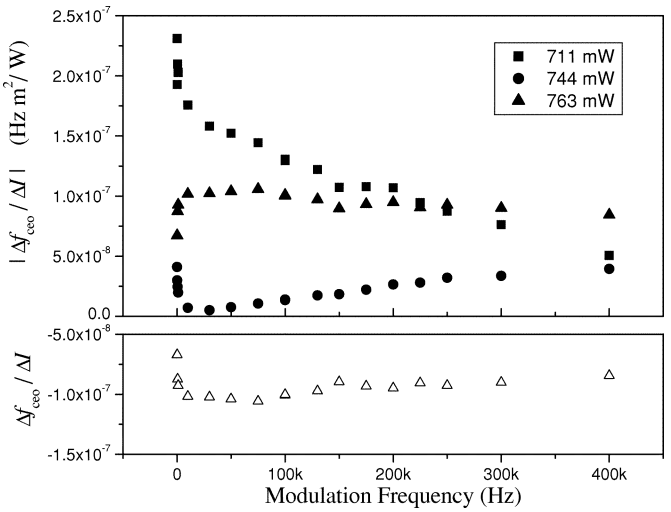

Fig. 5. Dynamic response (transfer function) of $f_{\rm ceo}$ with respect to laser power for the 750-MHz laser. Notice the change of the dynamic response when $f_{\rm ceo}$ goes through the turning point. Bottom panel shows the true response (inverted from the magnitude plot) for the 763-mW case.

$df_{\rm ceo}/dI$ for modulation frequencies from 10 Hz up to 400 kHz. The magnitude of the response for three different laser output powers of the 750-MHz laser is given in the top portion of Fig. 5. (The data were taken at a different time from the previous figures, and $f_{\rm ceo}$ reached a maximum at a higher laser power of ~775 mW instead of ~ 655 mW for previous figures.) The two data curves represented by squares and circles correspond to powers below the zero-crossing point of $df_{\rm ceo}/dI$ $(df_{\rm ceo}/dI > 0)$. The third data set represented by triangles corresponds to $df_{\rm ceo}/dI < 0$. The actual amplitude response for this last data set is shown in the bottom panel of Fig. 5. It is clear for Fourier frequencies below 1 kHz there is a steep rise in response toward dc, which we attribute to thermal effects in the Ti:s crystal. Above 1 kHz the response curve is roughly flat, at least up to the measured frequency range of 400 kHz. It is interesting to note that while the fast response of $df_{\rm ceo}/dI$ does change sign following $df_{\rm ceo}/dI$, the sign of the thermal response is unaffected by the zero crossing of $df_{\rm ceo}/dI$. This can explain why the response magnitude of $df_{\rm ceo}/dI$ approaches zero when the Fourier frequencies approach dc in the case of $df_{\rm ceo}/dI < 0$. An increased positive thermal response partially cancels the negative response of $df_{\rm ceo}/dI$ related to mode-locking pulse dynamics.

IV. Investigation of Lineshape of Carrier-Envelope Offset Frequency

The lineshape and width of the carrier-envelope offset frequency are shown in the top portion of Fig. 6 for various average output powers of the 750-MHz laser. The values of $f_{\rm ceo}$ associated with these various lineshapes are measured with a spectrum analyzer as the laser power is increased, representing a dc measurement of the frequency versus laser power. In the bottom panel of the figure are the experimental values of $df_{\rm ceo}/dI$ versus output power obtained with an intensity modulation at 10 kHz. From the study presented in Fig. 5, it is evident that if the value of $df_{\rm ceo}/dI$ obtained at 10-kHz modulation is zero, then the dc measurement of $df_{\rm ceo}/dI$ will produce a positive value since the thermal response is positive. Therefore, the dc measurement will determine that $df_{\rm ceo}/dI$ reaches a zero value at a higher power, where a 10-kHz modulation measurement already yields $df_{\rm ceo}/dI < 0$. It is seen from the lineshapes in Fig. 6 that the phase noise

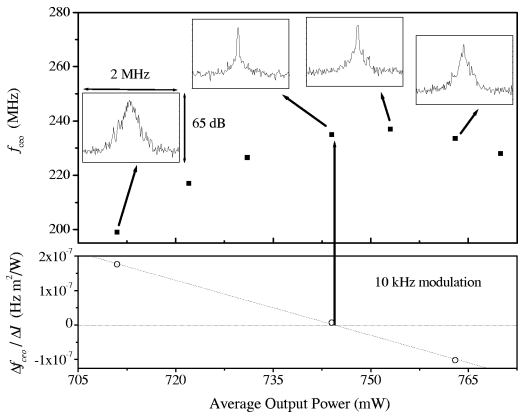

Fig. 6. Top: linewidth of $f_{\rm ceo}$ around the turning point $(\Delta f_{\rm ceo}/\Delta I = 0)$ in the 750-MHz laser with corresponding center frequencies obtained at dc. Bottom: $\Delta f_{\rm ceo}/\Delta I$ obtained at 10-kHz modulation.

associated with $f_{\rm ceo}$ increases dramatically when $df_{\rm ceo}/dI$ deviates from zero. The linewidth of $f_{\rm ceo}$ is at a minimum when $df_{\rm ceo}/dI$, as measured by the 10-kHz modulation and detection, crosses zero (not when the dc measured $f_{\rm ceo}$ reaches a maximum). This is easy to interpret since at the zero-crossing point of $df_{\rm ceo}/dI$, the phase variation of $f_{\rm ceo}$ is least sensitive to pulse intensity fluctuations, which appear to be the dominant source of noise for $f_{\rm ceo}$. This can be verified by considering the root-mean-square power fluctuations of the pump, provided by the pump laser manufacturer. A value of 0.02% of rms power fluctuations for the pump laser is given, which can be converted into frequency noise with the known coefficients of the dependence of $f_{\rm ceo}$ on the average Ti:s laser output power and the dependence of this average output power on the pump power. For the first point in Fig. 6 at 197 MHz, this conversion yields an rms frequency noise of ~200 kHz. In comparison, the measured width of the lineshape in Fig. 6 for this point is ~500 kHz. For the last linewidth shown in Fig. 6, the power fluctuations of the pump predict rms frequency noise of ~100 kHz, half that predicted for the first point. Indeed, the measured linewidth is ~300 kHz, roughly half that measured for the first

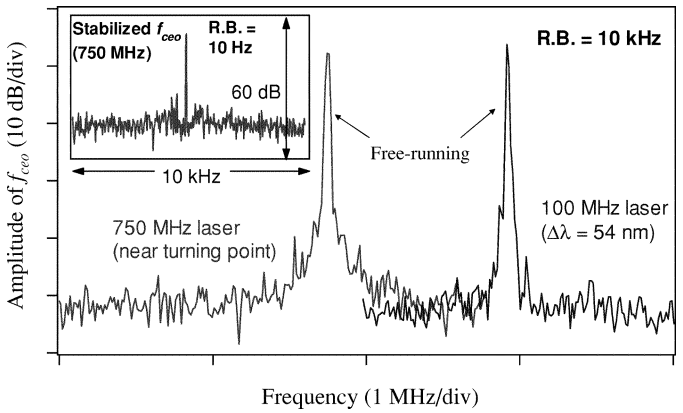

Fig. 7. Comparison of $f_{\rm ceo}$ linewidth between the 100- and 750-MHz lasers. $f_{\rm ceo}$ linewidth is nearly independent of the pulse intensity for the 100-MHz laser, while the narrowest $f_{\rm ceo}$ lineshape is shown for the 750-MHz laser. Inset shows the resolution-limited linewidth of the stabilized $f_{\rm ceo}$ for the 750-MHz laser.

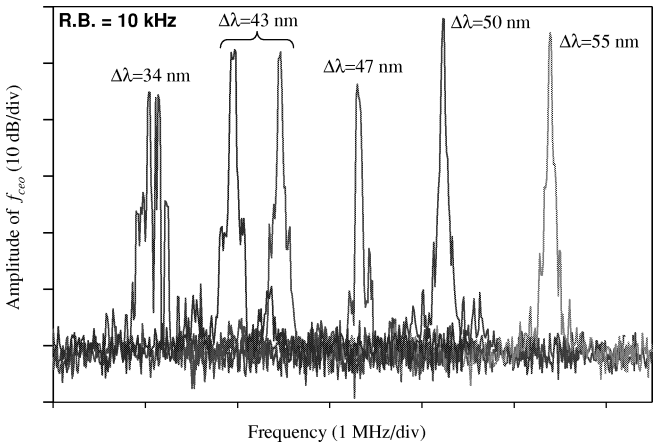

Fig. 8. Linewidths of $f_{\rm ceo}$ for the 100-MHz laser corresponding to various pulse spectrum bandwidths.

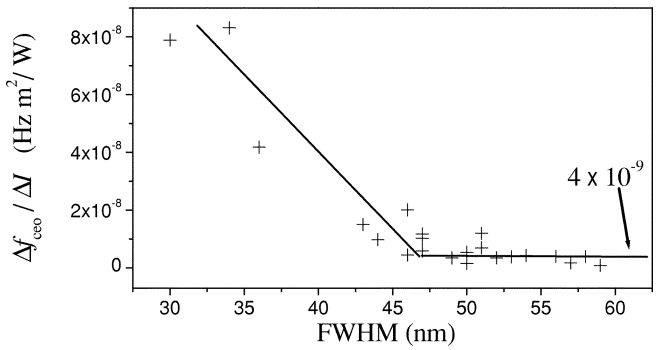

Fig. 9. Dependence of $\Delta f_{\rm ceo}/\Delta I$ on laser bandwidth for the 100-MHz laser.

point. The linewidths predicted solely by power fluctuations of the pump laser are in rough agreement with those measured.

In experiments involved with stabilization of $f_{\rm ceo}$, the 750-MHz laser is operated near the zero-crossing point of $df_{\rm ceo}/dI$. Under this condition, it is possible to phase lock $f_{\rm ceo}$ to a highly stable rf signal and achieve a linewidth basically of that of the rf reference. Shown in the inset in Fig. 7 is such a stabilized $f_{\rm ceo}$ signal, with a linewidth approaching 10-mHz level (not resolved by the resolution bandwidth shown in the figure). The phase locked loop is implemented with the laser pump power as the feedback actuator. On the other hand, if $df_{\rm ceo}/dI$ is tuned away from zero, it becomes increasingly difficult to phase lock $f_{\rm ceo}$ to a rf reference for the 750-MHz laser.

In contrast to this behavior, the 100-MHz laser system typically displays a free-running (no feedback) $f_{\rm ceo}$ linewidth that is comparable to or narrower than the best values for the free-running 750-MHz laser, as shown in Fig. 7. In order to understand the underlying physical mechanisms responsible for this difference in behavior, we study the intensity dependence of the 100-MHz laser system as the prism insertion is varied. The insertion changes both the width of the pulse spectrum and decreases the magnitude of the net cavity GDD. Shown in Fig. 8 are the linewidths of $f_{\rm ceo}$ for the 100-MHz system corresponding to various pulse spectral widths [full-width at half-maximum (FWHM)]. From these data, it appears that the $f_{\rm ceo}$ linewidth decreases as the width of the pulse spectrum increases, until the spectral width reaches about 47 nm. For spectral widths broader than $\sim$47 nm, the $f_{\rm ceo}$ linewidth in the 100-MHz laser is nearly constant. This observation is confirmed by the results shown in Fig. 9 for $df_{\rm ceo}/dI$ measured as a function of the FWHM of the pulse spectrum. An interesting threshold behavior is observed, where $df_{\rm ceo}/dI$ decreases sharply with increasing spectral bandwidth, again up to a bandwidth of $\sim$ 47 nm. For broader spectra, $df_{\rm ceo}/dI$ remains unchanged, at a value of $\sim 4 \times 10^{-9}$[Hz m^{2}W^{-1}]. The broader spectral bandwidth and corresponding decrease in the magnitude of the net cavity GDD both reduce the intensity dependence of $f_{\rm ceo}$ by reducing the magnitude of $\partial\omega_c/\partial I$ and $\partial(v_g^{-1})/\partial\omega_c$, respectively. The observations made in the 100-MHz laser system are thus consistent with those from the 750-MHz laser; a decrease in the magnitude of the intensity dependent spectral shift and/or net cavity GDD reduces the coupling of $f_{\rm ceo}$ to intensity fluctuations, thereby minimizing the corresponding free-running linewidth of $f_{\rm ceo}$. The fact that for all recorded pulse bandwidths shown in Fig. 9, the magnitude of $df_{\rm ceo}/dI$ for the 100-MHz laser is approximately ten times smaller than the corresponding value for the 750 MHz system, as shown in Fig. 4, explains why the $f_{\rm ceo}$ linewidth for the 100-MHz system is, in general, smaller than that of the 750-MHz laser. The dependence of the dynamics of the 750-MHz laser on the pulse bandwidth could not be studied since its bandwidth cannot be changed significantly for this prismless system.

V. Conclusion

Our study of the dynamics of $f_{\rm ceo}$ and $f_{\rm rep}$ for passively mode-locked Ti:sapphire systems confirms a connection between the dependence of $f_{\rm ceo}$ and $f_{\rm rep}$ on the laser intensity and the intensity-related shift of the laser pulse spectrum. It is seen that the signs of $df_{\rm ceo}/dI$ and $df_{\rm rep}/dI$ are correlated with that of $\partial\omega_c/\partial I$, and a model attributing the changes in $f_{\rm ceo}$ and $f_{\rm rep}$ to the spectral shift is consistent with the experimental data. When the intensity-related spectral shift is minimized at the optimum value of the pump power for the 750-MHz laser, the dependence of $f_{\rm ceo}$ on laser intensity is minimized. For the 100-MHz laser, the intensity dependence is diminished as the spectrum is broadened, accompanied by a decrease in the

magnitude of the net cavity GDD. The varying dependence of the pulse spectrum on laser intensity is being investigated. One possible contribution is a Raman-induced shift [21]. Another factor which could act to shift the laser spectrum is an offset between the gain band and loss band of the cavity. An increase in the pulse intensity, resulting in a decrease in the gain due to saturation, would shift the net gain profile of the cavity, thereby shifting the pulse spectrum [22]. This offers an explanation for the minimization of the intensity dependence of $f_{\rm ceo}$ for the 100-MHz laser when the pulse bandwidth exceeds $\sim$ 47 nm, since a broad bandwidth limits the amount of spectral shift that can occur. In addition, the decrease in the magnitude of the net cavity GDD, which accompanies the broadening of the spectral bandwidth for the 100-MHz laser, diminishes the effect of a spectral shift. Therefore, it is expected that systems with a larger magnitude of net cavity GDD have a stronger coupling to intensity fluctuations. The large negative GDD of the 750-MHz laser, which was found to be ~ -400 fs^2 from the values of $\partial(v_g^{-1})/\partial\omega_c$ calculated from the data in Fig. 4, would explain the larger dependence of $f_{\rm ceo}$ on the intensity compared to the 100-MHz laser. A system with near-zero net cavity GDD, as in a dispersion-managed mode-locked laser [23], should be least susceptible to intensity noise of the laser. In fact, in such systems utilizing prism pairs to achieve near-zero net cavity GDD it has been observed that there is no correlation between amplitude fluctuations of the laser and $f_{\rm ceo}$ [24]. Within our lab it has been noted that utilizing the pump power to stabilize $f_{\rm ceo}$ increases the amplitude noise of such lasers. The intensity must be changed dramatically to affect $f_{\rm ceo}$, since there is not strong coupling between the intensity of the laser and $f_{\rm ceo}$. This is in contrast to prismless systems with fixed nonzero GDD, where the fluctuations in $f_{\rm ceo}$ are found to be directly related to variations in the pulse intensity [25]. Because of these different behaviors, it is important to tailor the stabilization scheme to the laser system in use.

APPENDIX

In order to derive the intensity dependence of $f_{\rm rep}$ and $f_{\rm ceo}$, differentiate the expressions for $f_{\rm rep}$ and $f_{\rm ceo}$ with respect to I, yielding

$$\frac{df_{\rm rep}}{dI} = \frac{1}{l_c}\frac{dv_g}{dI} \tag{1a}$$

$$\frac{df_{\rm ceo}}{dI} = \frac{1}{2\pi}\frac{\partial\omega_c}{\partial I}\left(1-\frac{v_g}{v_p}\right) + \frac{\omega_c}{2\pi}\frac{v_g}{v_p}\left(\frac{1}{v_p}\frac{dv_p}{dI}-\frac{1}{v_g}\frac{dv_g}{dI}\right). \tag{1b}$$

Now, v_g is a function of both ω_c (which depends on I) and of I explicitly (through $\overline{n}$). Therefore

$$\frac{d}{dI}\left(\frac{1}{v_g}\right) = \frac{\partial\omega_c}{\partial I}\frac{\partial}{\partial\omega_c}\left(\frac{1}{v_g}\right) + \frac{1}{c}\frac{\partial}{\partial I}\left(\overline{n}_0+\overline{n}_2 I+\omega_c\left(\frac{d\overline{n}_0}{d\omega}\right)_{\omega_c} + \omega_c I\left(\frac{d\overline{n}_2}{d\omega}\right)_{\omega_c}\right)$$

$$= \frac{\partial\omega_c}{\partial I}\frac{\partial}{\partial\omega_c}\left(\frac{1}{v_g}\right) + \frac{1}{c}\left(\overline{n}_2+\omega_c\left(\frac{d\overline{n}_2}{d\omega}\right)_{\omega_c}\right). \tag{4}$$

The phase velocity v_p is also a function of both ω_c ($\overline{n}$ depends on ω_c through dispersion) and I

$$\frac{d}{dI}\left(\frac{1}{v_p}\right) = \frac{1}{c}\left[\frac{\partial\omega_c}{\partial I}\frac{\partial\overline{n}}{\partial\omega_c}+\frac{\partial}{\partial I}\left(\overline{n}_0+\overline{n}_2 I\right)\right] = \frac{1}{c}\left[\frac{\partial\omega_c}{\partial I}\frac{\partial\overline{n}}{\partial\omega_c}+\overline{n}_2\right]. \tag{5}$$

Rewriting the expression for $df_{\rm rep}/dI$ and plugging in (4) gives the dependence of $f_{\rm rep}$ on I

$$\frac{df_{\rm rep}}{dI} = -\frac{v_g^2}{l_c}\frac{d}{dI}\left(\frac{1}{v_g}\right) = -\frac{1}{l_c}\frac{v_g^2}{c}\left[\overline{n}_2+\omega_c\left(\frac{d\overline{n}_2}{d\omega}\right)_{\omega_c} + c\frac{\partial\omega_c}{\partial I}\frac{\partial}{\partial\omega_c}\left(\frac{1}{v_g}\right)\right]. \tag{2}$$

The same can be done for $df_{\rm ceo}/dI$ using (4) and (5)

$$\frac{df_{\rm ceo}}{dI} = \frac{1}{2\pi}\frac{\partial\omega_c}{\partial I}\left(1-\frac{v_g}{v_p}\right) + \frac{\omega_c}{2\pi}\frac{v_g}{v_p}\left(-v_p\frac{d}{dI}\left(\frac{1}{v_p}\right)+v_g\frac{d}{dI}\left(\frac{1}{v_g}\right)\right)$$

$$= \frac{1}{2\pi}\frac{\partial\omega_c}{\partial I}\left[\left(1-\frac{v_g}{v_p}\right)-\frac{\omega_c v_g}{c}\frac{\partial\overline{n}}{\partial\omega_c}+\frac{\omega_c v_g^2}{v_p}\frac{\partial}{\partial\omega_c}\left(\frac{1}{v_g}\right)\right] + \frac{\omega_c}{2\pi c}\frac{v_g}{v_p}\left[\overline{n}_2\left(v_g-v_p\right)+v_g\omega_c\left(\frac{d\overline{n}_2}{d\omega}\right)_{\omega_c}\right]. \tag{6}$$

The last term in brackets can be rearranged, using the expressions for v_g and v_p and expanding $\overline{n}$

$$\left[\overline{n}_2\left(v_g-v_p\right)+v_g\omega_c\left(\frac{d\overline{n}_2}{d\omega}\right)_{\omega_c}\right] = v_g\left[\overline{n}_2\left(1-\frac{\overline{n}+\omega_c\left(\frac{d\overline{n}}{d\omega}\right)_{\omega_c}}{\overline{n}}\right)+\omega_c\left(\frac{d\overline{n}_2}{d\omega}\right)_{\omega_c}\right]$$

$$= \frac{-v_g}{\overline{n}}\omega_c\overline{n}_2\left(\left(\frac{d\overline{n}_0}{d\omega}\right)_{\omega_c}+I\left(\frac{d\overline{n}_2}{d\omega}\right)_{\omega_c}\right) + \frac{v_g}{\overline{n}}\omega_c\left(\overline{n}_0+\overline{n}_2 I\right)\left(\frac{d\overline{n}_2}{d\omega}\right)_{\omega_c}$$

$$= \frac{v_g}{\overline{n}}\omega_c\left[-\overline{n}_2\left(\frac{d\overline{n}_0}{d\omega}\right)_{\omega_c}+\overline{n}_0\left(\frac{d\overline{n}_2}{d\omega}\right)_{\omega_c}\right]. \tag{7}$$

Substituting this expression into (6), one obtains the dependence of $f_{\rm ceo}$ on I

$$\frac{df_{\rm ceo}}{dI} = \frac{\omega_c^2}{2\pi}\frac{v_g^2}{c^2}\left[\overline{n}_0\left(\frac{d\overline{n}_2}{d\omega}\right)_{\omega_c}-\overline{n}_2\left(\frac{d\overline{n}_0}{d\omega}\right)_{\omega_c}\right]+\frac{1}{2\pi}\frac{\partial\omega_c}{\partial I} \times\left[\left(1-\frac{v_g}{v_p}\right)+\frac{\omega_c v_g^2}{v_p}\frac{\partial}{\partial\omega_c}\left(\frac{1}{v_g}\right)-\frac{\omega_c v_g}{c}\frac{\partial\overline{n}}{\partial\omega_c}\right]. \tag{3}$$

ACKNOWLEDGMENT

The authors would like to thank D. Jones and T. Fortier for their generous technical help and F. Kärtner, E. Ippen, and H. Haus for useful discussions.

REFERENCES

[1] T. Udem, J. Reichert, R. Holzwarth, and T. W. Hänsch, *Phys. Rev. Lett.*, vol. 82, p. 3568, 1999.
[2] J. Ye, T. H. Yoon, J. L. Hall, A. A. Madej, J. E. Bernard, K. J. Siemsen, L. Marmet, J.-M. Chartier, and A. Chartier, *Phys. Rev. Lett.*, vol. 85, p. 3797, 2000.
[3] L. Xu, C. Spielmann, A. Poppe, T. Brabec, F. Krausz, and T. W. Hänsch, *Opt. Lett.*, vol. 21, p. 2008, 1996.
[4] D. J. Jones, S. A. Diddams, J. K. Ranka, A. Stentz, R. S. Windeler, J. L. Hall, and S. T. Cundiff, *Science*, vol. 288, p. 635, 2000.
[5] A. Apolonski, A. Poppe, G. Tempea, C. Spielmann, T. Udem, R. Holzwarth, T. W. Hänsch, and F. Krausz, *Phys. Rev. Lett.*, vol. 85, p. 740, 2000.
[6] S. A. Diddams, T. Udem, J. C. Bergquist, E. A. Curtis, R. E. Drullinger, L. Hollberg, W. M. Itano, W. D. Lee, C. W. Oates, K. R. Vogel, and D. J. Wineland, *Science*, vol. 293, p. 825, 2001.
[7] J. Ye, L. S. Ma, and J. L. Hall, *Phys. Rev. Lett.*, vol. 87, p. 270 801, 2001.
[8] J. D. Jost, J. L. Hall, and J. Ye, *Opt. Express*, vol. 10, p. 515, 2002.
[9] L.-S. Ma, R. K. Shelton, H. C. Kapteyn, M. M. Murnane, and J. Ye, *Phys. Rev. A*, vol. 64, p. 021 802, 2001.
[10] R. K. Shelton, L. S. Ma, H. C. Kapteyn, M. M. Murnane, J. L. Hall, and J. Ye, *Science*, vol. 293, p. 1286, 2001.
[11] M. T. Asaki, C. P. Huang, D. Garvey, J. P. Zhou, H. C. Kapteyn, and M. M. Murnane, *Opt. Lett.*, vol. 18, p. 977, 1993.
[12] A. Bartels, T. Dekorsy, and H. Kurz, *Opt. Lett.*, vol. 24, p. 996, 1999.
[13] J. K. Ranka, R. S. Windeler, and A. J. Stentz, *Opt. Lett.*, vol. 25, p. 25, 2000.
[14] J. Reichert, R. Holzwarth, T. Udem, and T. W. Hänsch, *Opt. Comm.*, vol. 172, p. 59, 1999.
[15] H. R. Telle, G. Steinmeyer, A. E. Dunlop, J. Stenger, D. H. Sutter, and U. Keller, *Appl. Phys. B*, vol. 69, p. 327, 1999.
[16] T. Brabec and F. Krausz, *Rev. Mod. Phys.*, vol. 72, p. 545, 2000.
[17] A. Baltuska, T. Udem, M. Uiberacker, M. Hentschel, E. Goulielmakis, C. Gohle, R. Holzwarth, V. S. Yakoviev, A. Scrinzi, T. W. Hansch, and F. Krausz, *Nature*, vol. 421, p. 611, 2003.
[18] R. J. Jones and J. C. Diels, *Phys. Rev. Lett.*, vol. 86, p. 3288, 2001.
[19] J. Ye, S. T. Cundiff, S. Foreman, T. M. Fortier, J. L. Hall, K. W. Holman, D. J. Jones, J. D. Jost, H. C. Kapteyn, K. A. H. V. Leeuwen, L.-S. Ma, M. M. Murnane, J.-L. Peng, and R. K. Shelton, *Appl. Phys. B*, vol. 74, p. S-27, 2002.
[20] F. W. Helbing, G. Steinmeyer, U. Keller, R. S. Windeler, J. Stenger, and H. R. Telle, *Opt. Lett.*, vol. 27, p. 194, 2002.
[21] H. A. Haus, I. Sorokina, and E. Sorokin, *J. Opt. Soc. Amer. B*, vol. 15, p. 223, 1998.
[22] V. L. Kalashnikov, E. Sorokin, and I. T. Sorokina, *J. Opt. Soc. Amer. B*, vol. 18, p. 1732, 2001.
[23] Y. Chen, F. X. Kärtner, U. Morgner, S. H. Cho, H. A. Haus, E. P. Ippen, and J. G. Fujimoto, *J. Opt. Soc. Amer. B*, vol. 16, p. 1999, 1999.
[24] U. Morgner, R. Ell, G. Metzler, T. R. Schibli, F. X. Kärtner, J. G. Fujimoto, H. A. Haus, and E. P. Ippen, *Phys. Rev. Lett.*, vol. 86, p. 5462, 2001.
[25] A. Poppe, R. Holzwarth, A. Apolonski, G. Tempea, C. Spielmann, T. W. Hänsch, and F. Krausz, *Appl. Phys. B*, vol. 72, p. 373, 2001.

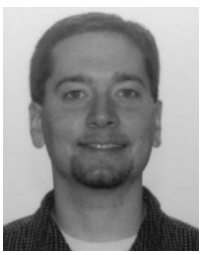

Kevin W. Holman was born in Louisville, KY, in 1978. He received the B.S. degree in physics and mathematics from Purdue University, West Lafayette, IN, in 2000. He is currently working toward the Ph.D. in physics at the University of Colorado, Boulder.

At the present time, he is studying ultrafast optical frequency combs in the group of Prof. Jun Ye at JILA, within the University of Colorado. He is investigating the use of a mode-locked Ti:sapphire laser in the development of an optical clock. Also, he is working to transfer the stability of the Ti:sapphire comb to that of a mode-locked diode laser for transfer of the comb through optical fiber.

R. Jason Jones was born in Sioux Falls, SD, in 1972. He received the B.S. degree in physics from Bethel College, St. Paul, MN, in 1994 and the Ph.D. degree in optical science from the University of New Mexico, Albuquerque, in 2001.

His graduate work focused on the use of stable Fabry–Pérot cavities for both intracavity dispersion measurements and stabilization of femtosecond lasers for optical frequency measurements. He is currently a Postdoctoral Research Associate at JILA (a joint institute of the University of Colorado and the National Institute of Standards and Technology), Boulder, CO.

Adela Marian was born in Bucharest, Romania, in 1976. She received the B.S. degree in physics from the University of Bucharest, Bucharest, Romania, in 1998. She is currently working toward the Ph.D. degree in physics at the University of Colorado, Boulder.

At the present time she is doing research in the group of Prof. Jun Ye at JILA (a joint institute of the National Institute of Standards and Technology and the University of Colorado), Boulder. She is using a phase-coherent wide-bandwidth femtosecond laser comb to induce and study two-photon transitions in cold Rb atoms. She is also working on an experiment in high-precision semiconductor spectroscopy using cavity ringdown techniques.

Steven T. Cundiff received the B.A. degree in physics from Rutgers University, New Brunswick, NJ, in 1985. In 1992, he received the Ph.D. degree in applied physics from the University of Michigan, Ann Arbor.

He worked for two years at SciTec, Inc. in Princeton, N.J. In 1993 and 1994, he was a von Humboldt post-doctoral Fellow at Philipps University, Marburg, Germany. He was a post-doctoral Member of Technical Staff in the Advanced Photonics Research Department, Bell Labs, Lucent Technologies, Holmdel, NJ, from 1995 to 1997. Currently, he is a Physicist in the Quantum Physics Division, National Institute of Standards and Technology (NIST) and a Fellow of JILA, a joint institute between NIST and the University of Colorado, Boulder. He is also an Adjoint Faculty Member in the Department of Physics and Department of Electrical and Computer Engineering, University of Colorado.

Jun Ye born on Nov. 7, 1967, in Shanghai, China. He received the Ph.D. degree from the University of Colorado, Boulder, in 1997.

He is a fellow of JILA (a joint institute of the National Institute of Standards and Technology and the University of Colorado), Boulder. He leads a team of researchers who are working in areas including high-precision measurement, high-resolution and ultrasensitive laser spectroscopy, optical frequency metrology, ultrafast optics, cooling and trapping of atoms and molecules, and quantum dynamics in optical and atomic physics. He has co-authored over 100 technical papers and is a recipient of a number of awards from professional societies and agencies.